

Callus Thickness Determination Adjuvant to Tissue Oximetry Imaging

Gennadi Saiko^{1,2} 

¹Swift Medical Inc., 1 Richmond St. W., Toronto, Canada

²Ryerson University, Toronto, Canada

Keywords: Diabetic Foot Ulcer, Oximetry, Turbid Tissues.

Abstract: Introduction: Corns and calluses are thickened skin due to repeated friction, pressure, or other irritation. While in many cases, calluses are harmless, if not removed timely, they may lead to skin ulceration or infection. Thus, the removal of calluses is an essential part of surgical debridement. Often, healthcare professionals experience problems with their identification. This study aims to develop an approach for callus thickness determination using hyperspectral imaging. Methods: Based on the two-layer tissue model developed by Yudovsky D et al., 2010, we have developed a computationally simple way of extracting the epithelial thickness from spectral measurements of skin reflection. We have performed a numerical evaluation of the proposed algorithm: generated the reflectance spectrum using the two-layer model, added noise, and reconstructed the epidermal thickness L using the proposed method. To evaluate performance, we have used the following parameters: thickness of the epithelium: 0.1-2mm, dermal blood concentration: 0.2%, 3%, and 7%, blood oxygen saturation: 60%, 80%, and 99%. Results: We have found that the model reasonably well extracts epidermal thickness L in the 0.1-1.5mm range. Beyond that, the reflectance signal does not bring information about underlying layers. The most significant factor, which impacts estimation, is the scattering coefficient of the epidermis. Other factors can be mainly ignored. Conclusions: The proposed model can be easily implemented in image processing algorithms for hyperspectral/multispectral imaging systems.

1 INTRODUCTION

Corns and calluses are thickened skin areas due to repeated friction, pressure, or other irritation. They are created by the accumulation of undifferentiated keratinocytes in the outermost layer of skin. Though the cells of calluses are dead, they are resistant to mechanical and chemical impacts due to extensive networks of cross-linked proteins and hydrophobic keratin intermediate filaments containing many disulfide bonds. Calluses are the natural reaction to irritation of the palmar or plantar skin. Too much friction occurring too fast for the skin to develop a protective callus will cause a blister or abrasion instead.

Several risk factors like foot deformities (e.g., bunions, hammertoe) and not wearing socks or protective gloves facilitate callus formation.


While in many cases, calluses are harmless, if not removed timely, they may lead to skin ulceration

or infection, which is of particular importance for patients with diabetes. They can also cause the patient to try offload the affected painful area, placing excessive stress on the asymptomatic side.

Thus, the removal of calluses is an essential part of surgical debridement. However, in many cases, healthcare professionals experience problems with their identification. While corns are typically clearly visible, calluses are often unsightly. Consequently, some areas of dead skin can be missed during debridement.

Therefore, a clinical tool that will help identify suspected areas would be of great clinical utility.

In (Yudovsky, 2010) the authors proposed estimating blood saturation, melanin content, and epidermis thickness from spectral diffuse reflectance measurements. Using Monte Carlo simulations, the authors solved the radiative transfer equation and applied an inverse method to retrieve physiological parameters. However, the technique is suitable

 <https://orcid.org/0000-0002-5697-7609>

mainly for a single-point assessment and cannot be extended to imaging geometry due to computational complexity.

This problem is closely related to the maximal detection depth problem discussed analytically (Saiko, 2012) and using Monte Carlo (Saiko, 2014).

This study aims to develop an approach for callus thickness determination using hyperspectral or multispectral imaging

2 METHODS

2.1 Tissue Model

The skin is a multi-layer structure. Typically, it is subdivided into three primary layers: epidermis, dermis, and subcutaneous tissue. However, each of these layers can be split into several respective sub-layers.

However, considering the spectrum's visible range, the light penetration depth does not exceed 2mm, and subcutaneous tissue does not contribute much to the reflectance. Thus, in this case, we can consider the skin as a two-layer structure: the bloodless epidermis and underlying, blood-containing tissue, which has optical properties of the dermis.

We will approximate the epidermis as a slab of thickness L_1 . In the normal case, the epidermis is not more than 100-120 μ m thick; however, it can be several millimeters thick in the callus. Such as light does not penetrate more than 2mm into the dermis; we can approximate it as a semi-infinite layer.

2.2 Optical Tissue Model

Thus, we can model the skin as a two-layer structure, where a slab with optical parameters (μ_{a1}, μ'_{s1}) and thickness L_1 covers a semi-space with optical parameters (μ_{a2}, μ'_{s2}) . Here and after that, indexes 0, 1, and 2 refer to the air, epidermal, and underlying tissues, respectively. Thus, our ultimate goal will be to find L_1 from optical measurements.

In (Yudovsky, 2009) the authors investigated such model using a two-flux Kubelka-Munk approach with mismatched external boundary and matched interlayer interface and found that the reflectance of such a two-layer model can be expressed as

$$R = R'(R_-(n_1, \omega_1) - R_-(n_1, \omega_2)) + R_-(n_1, \omega_2) \quad (1)$$

Here $R_-(n, \omega)$ is the reflectance of the semi space with the index of refraction n and reduced albedo ω ($\omega = \mu'_s / (\mu'_s + \mu_a)$), and R' is the "reduced reflectance," which varies in the range from 0 to 1.

The reflectance of the semi space with mismatches boundary can be written as (Saunderson, 1942)

$$R_- = r_{01} + \frac{(1 - r_{01})(1 - r_{10})R_d}{1 - r_{10}R_d} \quad (2)$$

Here r_{01} is the specular reflectance for the light coming from air to the tissue, r_{10} is the specular reflectance of the light coming from the tissue into the air, R_d is the diffuse reflectance of the tissue. The diffuse reflectance of the semi space with optical properties (μ_a, μ'_s) can be found using the Kubelka-Munk (K-M) model

$$R_d = a - \sqrt{a^2 - 1} \quad (3)$$

Where $a = (S + K) / S$. In (van Gemert, 1987), the authors expressed K-M absorption and scattering coefficients K and S through μ_a and μ'_s .

While the reduced reflectance R' can be found analytically, a semi-empirical approach (Yudovsky, 2009) with fitting parameter a gives more accurate predictions of tissue reflectance

$$R' = \frac{\tanh(Y_1)}{1/\alpha + (1 - 1/\alpha)\tanh(Y_1)} \quad (4)$$

Here

$$Y_1 = \zeta(\mu_{a1} + \mu'_{s1})L_1 \quad (5)$$

where ζ is the root of the characteristic equation

$$\alpha = \frac{2\zeta}{\ln((1 + \zeta)/(1 - \zeta))} \quad (6)$$

2.3 Physiological Considerations

In the general case, the skin contains melanin located in the bottom, basal layer of the epidermis. However, there are two considerations why we can ignore its impact in the case of callus. Firstly, calluses are mainly located on plantar surfaces (sole and palm), which are melanin-free. Secondly, for other body locations, one can expect that the skin's normal processes are disrupted, so most likely, the skin will not form melanin protection in the case of the callus/corn. Thus, we can ignore melanin, which significantly simplifies our calculations.

In this case, we have the epidermal slab with quite universal optical characteristics, which are not affected by a skin type, and thus, should have low interpatient variability. So, we can tabulate its optical properties (μ_{a1} , μ'_{s1}).

The optical properties of the dermis are a little bit more tricky case. In the spectrum's visible range, they will be affected by blood, namely its concentration and composition (oxygenation). For the normal dermis, blood concentration is typically considered to be close to 3%. However, a callus may hide blood pools in some cases, where the blood concentration will be obviously higher. Furthermore, oxygenation of the blood varies from 97-99% for the arterial blood up to 60% for the venous blood. In the general case, the light samples both arterial and venous compartments, so the measured SO2 is somewhere between these values. However, to test the method, it is better to check the whole range.

2.4 Algorithm

The method can be described as the following:

1. Measure R at several wavelengths
2. Tabulate parameters (μ_{a1} , μ'_{s1}) and seed realistic n , α and (μ_{a2} , μ'_{s2}), e.g., healthy tissue
3. Calculate $R_d(\omega_1)$ and $R_d(\omega_2)$ using the K-M model (Eq.3)
4. Calculate $R_-(n, \omega_1)$ and $R_-(n, \omega_2)$ using Eq.2
5. Calculate R' :
$$R' = \frac{R - R_-(n, \omega_2)}{R_-(n, \omega_1) - R_-(n, \omega_2)}$$
6. Calculate Y_1 by solving Eq.4
7. Using tabulated values (μ_{a1} , μ'_{s1}) and ζ from Eq.6, find L_1 using Eq.5.
8. Update Y_1 , and recalculate R'
9. Calculate R_2 :
$$R_2 = \frac{R - R' R_1}{1 - R'}$$
10. Calculate R_{d2} by reversing Eq.2
11. Calculate K and S and then update (μ_{a2} , μ'_{s2})
12. Repeat steps 3-11 with updated (μ_{a2} , μ'_{s2}) if required

2.5 Parameters

2.5.1 Absorption

In the absence of melanin, the epidermis absorption can be modeled as the background absorption of human flesh (Jacques, 1996): $\mu_{a1} = \mu_{a,fl}$, where

$$\mu_{a,fl} = 7.84 \times 10^7 \lambda^{-3.255} \text{ [mm}^{-1}\text{]}. \text{ Here, the wavelength } \lambda \text{ is measured in [nm].}$$

The absorption of the dermis can be modeled as a combination of background-, oxyhemoglobin-, and deoxyhemoglobin related absorption

$$\mu_{a2} = (1-c)\mu_{a,fl} + c(SO2 * \mu_{a,HbO2} + (1-SO2) * \mu_{a,RHb}) \quad (7)$$

Here c is the blood concentration in the dermis, $SO2$ is the oxygen blood saturation, $HbO2$ and RHb refer to oxyhemoglobin and deoxyhemoglobin, respectively. Absorption coefficients for oxyhemoglobin- and deoxyhemoglobin are well known (Prahl, 2002). Blood typically occupies around 0.2-0.6% of the physical volume of the dermis (Lister, 2012). However, other groups report much higher values: up to 7% (Jacques, 1996).

2.5.2 Scattering

The reduced scattering coefficient for dermis and epidermis also follows a power law (Mourant, 1998): $\mu'_s \propto \lambda^{-k}$, with $k=1.3$. Therefore, we can set a reference value at a particular wavelength and simulate its dependence on the wavelength with this power law. In particular, we can assign values at 633nm (Meglinski, 2002) for the living epidermis ($\mu'_s=9\text{mm}^{-1}$) and reticular dermis ($\mu'_s=5\text{mm}^{-1}$), which represent the bulk of the tissue in healthy epidermis and dermis, respectively. However, for callus assessment, we can expect that the bulk of the callus is similar to the stratum corneum ($\mu'_s=14\text{mm}^{-1}$). Thus, we can write $\mu'_{s1} = 6.1 \times 10^4 \lambda^{-1.3}$ and $\mu'_{s2} = 2.2 \times 10^4 \lambda^{-1.3}$, respectively.

2.5.3 Index of Refraction

The index of refraction measurements in the human skin was summarized in (Bashkatov, 2011). The measurements in the visible spectrum range give their values from 1.433 to 1.449 for the epidermis (Ding, 2006). In particular, we can set 1.448, 1.447, and 1.433 for 442, 532, and 633nm, respectively. The dermis contains more water. Thus, its index of refraction is slightly (typically by 0.01-0.05 (Ding, 2006)) less, which will result in almost negligible scattering on the dermis/epidermis interface ($\ll 1\%$). Thus, we will ignore this difference and set $n_2=n_1$.

2.5.4 Noise

To make our synthetic spectrum more realistic, we have added noise to the simulated spectra. If we consider a consumer-grade camera with an 8-bit

depth, we can estimate that the measurement's experimental error for this camera is $1/(2^8 - 1) \approx 0.004$. Based on these assumptions, the realistic noise is $\sigma=0.001$. However, we have added Gaussian noise with $\mu=0$ and $\sigma=0.004$.

2.6 Test Scenarios

Four optical parameters ($\mu_{a1}, \mu'_{s1}, \mu_{a2}, \mu'_{s2}$) can characterize the two-layer K-M model. These parameters can be further described by five tissue parameters: power-law values for ($\mu_{a1}, \mu'_{s1}, \mu'_{s2}$), blood concentration c , and blood oxygenation, SO_2 .

The most uncertain parameters in the experiment are the scattering coefficient of the epidermis ($\mu'_s=9\text{mm}^{-1}$ or 14mm^{-1} for living epidermis and stratum corneum, respectively), blood concentration in the dermis, c (0.2-7%), and blood oxygen saturation, SO_2 (60-99%).

We will keep other parameters (μ_{a1}, μ'_{s2}) fixed: $\mu_{a1} = 7.84 \times 10^7 \lambda^{-3.255}$ and $\mu'_{s2} = 2.2 \times 10^4 \lambda^{-1.3}$, respectively.

2.6.1 Seed Parameters

We have seeded the algorithm with the following parameters: scattering coefficient of the epidermis' $\mu'_{s1}=14\text{mm}^{-1}$ (stratum corneum), blood concentration in the dermis, $c = 3\%$, and blood oxygen saturation $SO_2=80\%$.

2.6.2 Test Parameters

We have selected the following values to evaluate the model: the scattering coefficient of the epidermis $\mu'_{s1}=9\text{mm}^{-1}$ and 14mm^{-1} . Blood concentration: 0.2%, 3%, and 7%. Oxygen saturation: 60%, 80%, and 99%.

The epidermis's thickness, L_1 , was 100, 200, 400, 600, 800, 1000, 1500 μm .

3 RESULTS

We have performed a numerical evaluation of the proposed algorithm. For these purposes, we generated the reflectance spectrum using the two-layer model (Eq.1), added noise and reconstructed the thickness L_1 using steps 2-7.

We sampled reflectance at 470, 540, and 630 nm to measure epidermal thickness, processed them using the algorithm, extracted L_1 for each

wavelength, and averaged them to get a single value L_1 . To calculate statistical values (mean and standard deviation), we repeated them five times for each thickness for each parameter set.

3.1 Dependence on Oxygenation

The dependence of the extracted thickness as a function of the actual thickness for various blood oxygenations (60, 80, 99%) is depicted in Fig. 1.

Other test parameters were as following scattering coefficient of the epidermis 14mm^{-1} , blood concentration: 3%.

It can be seen that the oxygenation barely impacts the results.

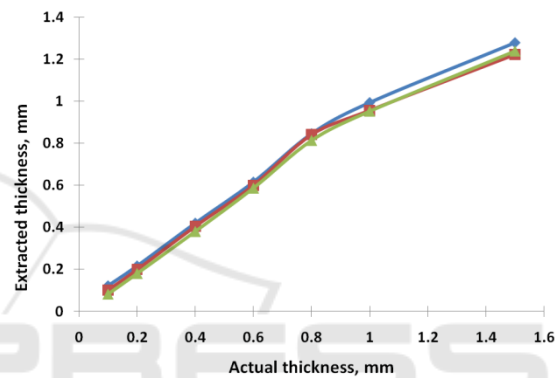


Figure 1: The extracted thickness as a function of the actual thickness for various SO_2 (60 (green triangle), 80 (red square), and 99 (blue rhomb) %). $\mu'_{s1}=14\text{mm}^{-1}$, $c=3\%$.

3.2 Dependence on Blood Content

The dependence of the extracted thickness as a function of the actual thickness for various blood concentrations (0.2, 3.0, and 7.0 %) is depicted in

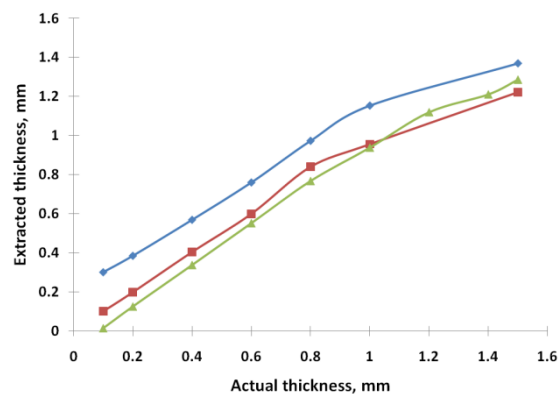


Figure 2: The extracted thickness as a function of the actual thickness for various blood concentrations (0.2 (blue rhomb), 3.0 (red square), and 7.0 (green triangle) %). $\mu'_{s1}=14\text{mm}^{-1}$, $SO_2=80\%$.

Fig. 2. Other test parameters were as following scattering coefficient of the epithelium 14mm^{-1} , blood oxygenation: 80%.

3.3 Dependence on Scattering Coefficient

The dependence of the extracted thickness as a function of the actual thickness for various scattering coefficients of the epithelium (14mm^{-1} and 9mm^{-1}) is depicted in Fig. 3.

Other test parameters were as following blood concentration: 3%, blood oxygenation: 80%.

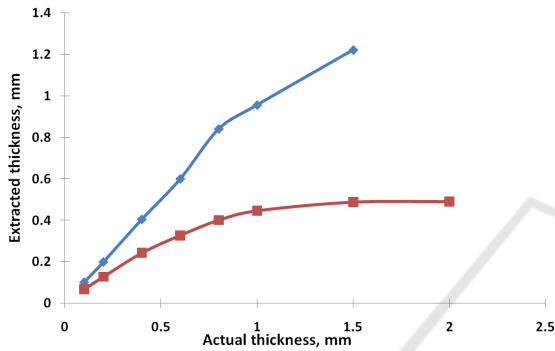


Figure 3: The dependence of the extracted thickness as a function of the actual thickness for various scattering coefficients of the epithelium (14mm^{-1} (blue rhomb) and 9mm^{-1} (red square)). $c=3\%$, $SO_2=80\%$.

3.4 Maximal Detected Thickness

To detect the maximal thickness, which can be identified by our method, we have performed emulation of reflectance spectra for tissues with maximal blood content (7%). In this case, we can expect that the impact of the underlying layer will be maximal.

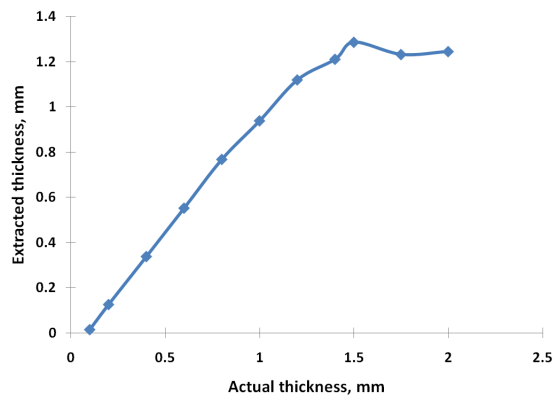


Figure 4: The dependence of the extracted thickness as a function of the actual thickness for maximal blood concentrations ($c=7.0\%$). $\mu'_{s,l}=14\text{mm}^{-1}$, $SO_2=80\%$.

The dependence of the extracted thickness as a function of the actual thickness for maximal blood concentrations ($c=7.0\%$) is depicted in Fig. 4. Other test parameters were as following: scattering coefficient of the epithelium 14mm^{-1} , blood oxygenation: 80%.

4 DISCUSSION

We have found that the model reasonably well extracts epidermal thickness L for the range of thicknesses 0.1-1.5mm. Beyond that, the reflectance signal does not bring information about underlying layers. In this case, the epidermis can be viewed as a semi-infinite layer.

We have found that SO_2 barely impacts results. So, in realistic scenarios, it can be ignored.

Blood content slightly impacts results. Underestimation of the blood content pushes the graph up (overestimates the thickness slightly). Overestimation of the blood content pulls the curve down (underestimate the thickness slightly). However, its effect for $L>0.4\text{mm}$ is relatively small and can be discarded for estimation purposes. For $L<0.3\text{mm}$, the error can be $>40\%$. However, it should be noted that our lower case scenario (0.2%) is significantly smaller than our seed value (3%). In realistic settings, it could be expected that the seed value could be selected closer to actual values, so its effect can be ignored.

The most significant factor, which impacts estimation, is the scattering coefficient of the epidermis. 30% error in evaluating the scattering coefficient (9mm^{-1} instead of 14mm^{-1}) leads to a significant underestimation of the thickness. It should be noted that for 0.1-0.8mm thickness, it can be corrected using the optical path: $L_{actual}\mu'_{s,l_{actual}} \approx L_{perceived}\mu'_{s,l_{seed}}$. However, in realistic conditions, one can expect that the callus consists of dead cells primarily, so it should not be an issue. However, this strong dependence underscores the importance of using realistic numbers.

The obtained maximal detection depth estimation agrees with the assessment of maximal defect detection depth developed in (Saiko, 2021) and elaborated in (Saiko, 2022a).

Speaking of the extension of the model to other scenarios, it should be mentioned that we excluded melanin from our model (see Section 2.3 for details). In most other cases it cannot be ignored. If

necessary, the melanin can be accounted for by a quasi-two layer model (Saiko, 2022b).

In the future, we plan to validate this approach in phantom experiments.

5 CONCLUSIONS

We have proposed an approach for optical callus thickness determination. Numerical simulations show that it can accurately detect epidermis thickness up to 1.5mm. Due to its computational simplicity, it can be easily implemented in image processing algorithms for multispectral and hyperspectral imaging systems

REFERENCES

- Yudovsky D, Pilon L, 2010, Rapid and accurate estimation of blood saturation, melanin content, and epidermis thickness from spectral diffuse reflectance., *Appl Opt.* 49(10):1707-19.
- Saiko G, Douplik A, 2012, Real-Time Optical Monitoring of Capillary Grid Spatial Pattern in Epithelium by Spatially Resolved Diffuse Reflectance Probe, *J. Innov. Opt. Health Scie.* 05 (02): 1250005.
- Saiko G, Pandya A, Schelkanova I, Sturmer M, Beckert RJ, Douplik A, 2014, Optical Detection of a Capillary Grid Spatial Pattern in Epithelium by Spatially Resolved Diffuse Reflectance Probe: Monte Carlo Verification, *IEEE J Sel. Top. Quant Electronics*, 20(2): 7000609
- Yudovsky D, Pilon L, 2009, Simple and accurate expressions for diffuse reflectance of semi-infinite and two-layer absorbing and scattering media. *Appl Opt.*; 48(35):6670-83.
- Saunderson JL, 1942, Calculation of the color of pigmented plastics, *J Opt Soc Amer*, 32(12):727-736.
- Van Gemert MJC, Star WM, 1987, Relations between the Kubelka-Munk and the transport equation models for anisotropic scattering, *Lasers Life Scie*, 1(98): 287-298.
- Jacques SL, Origins of tissue optical properties in the UVA, visible, and NIR regions, in *Advances in Optical Imaging and Photon Migration*, R. R. Alfano and J. G. Fujimoto, eds. (Optical Society of America, 1996), Vol. 2, pp. 364-370
- Prahl S, Optical absorption of hemoglobin, World Wide Web: <http://omlc.ogi.edu/spectra/hemoglobin/hemestruct/index.html>, 2002.
- Lister T, Wright PA, Chappell PH, 2012, Optical properties of human skin, *JBO* 17(9): 090901
- Mourant JR, Freyer JP, Hielscher AH, Eick AA, Shen D, Johnson TM, 1998, Mechanisms of light scattering from biological cells relevant to noninvasive optical-tissue diagnostics, *Appl Opt*, 37(16): 3586-3593.
- Meglinski IV, Matcher SJ, 2002, Quantitative assessment of skin layers absorption and skin reflectance spectra simulation in the visible and near-infrared spectral regions, *Physiol. Meas.* 23, 741-753.
- Bashkatov AN, Genina EA, Tuchin VN, 2011, Optical properties of skin, subcutaneous, and muscle tissues: A review, *J. Innov Opt Health Scie* 4(1): 9-38.
- Ding H, Lu JQ, Wooden WA, Kragel PJ, Hu X-H, 2006, Refractive indices of human skin tissues at eight wavelengths and estimated dispersion relations between 300 and 1600 nm, *Phys. Med. Biol.* 51, 1479-1489.
- Saiko G, Douplik A, Contrast Ratio during Visualization of Subsurface Optical Inhomogeneities in Turbid Tissues: Perturbation Analysis. In Proc of the 14th Int Joint Conf on Biomed Eng Systems and Technologies (BIOSTEC 2021) - v 2: BIOIMAGING, 94-102, DOI: 10.5220/0010374100940102
- Saiko G, Douplik A, Visibility of capillaries in turbid tissues: an analytical approach, *SN Comp. Scie* (submitted)
- Saiko G, Improved optical tissue model for tissue oximetry imaging applications, *Adv Exp Med Biol* (submitted)